



# Multi-machine scaling of the divertor peak heat flux and width for L-mode and H-mode discharges

A. Loarte <sup>a,\*</sup>, S. Bosch <sup>b</sup>, A. Chankin <sup>c</sup>, S. Clement <sup>c</sup>, A. Herrmann <sup>b</sup>, D. Hill <sup>d</sup>,  
K. Itami <sup>e</sup>, J. Lingertat <sup>c</sup>, B. Lipschultz <sup>f</sup>, K. McCormick <sup>b</sup>, R. Monk <sup>c</sup>,  
G.D. Porter <sup>d</sup>, M. Shimada <sup>e</sup>, M. Sugihara <sup>g</sup>

<sup>a</sup> *The NET Team, Max-Planck-Institut für Plasmaphysik, D-85748 Garching, Germany*

<sup>b</sup> *Max-Planck-Institut für Plasmaphysik, EURATOM Assoc., D-85748 Garching, Germany*

<sup>c</sup> *JET Joint Undertaking, Abingdon Oxon., OX14 3EA, UK*

<sup>d</sup> *Lawrence Livermore National Laboratory, P.O. Box 808, Livermore, CA 94550, USA*

<sup>e</sup> *JAERI, Naka Fusion Research Establishment, Ibaraki-ken 311-01, Japan*

<sup>f</sup> *Plasma Fusion Centre, MIT, Cambridge, MA 01239, USA*

<sup>g</sup> *ITER Joint Central Team, Joint Working Site, D-85748 Garching, Germany*

---

## Abstract

The ITER divertor power deposition database is described and analysed in this paper. The database contains experimental measurements from the major divertor experiments in L-mode and H-mode regimes. These measurements are used to derive multi-machine scaling laws for the peak divertor heat flux and width, particularly of their machine size dependence. The physical basis for these scalings is discussed and the laws obtained are used to extrapolate from existing experiments to the parameters expected in the ITER-EDA device. © 1999 Elsevier Science B.V. All rights reserved.

*Keywords:* Database; H-mode; IRTV; ITER; L-mode; Power deposition; Power peaking; SOL power; SOL thickness

---

## 1. Introduction

One of the main problems in the design of ITER is that of power loading on first wall materials. The predicted values of the power flux to the divertor surfaces in ITER are likely to exceed the limits set by engineering and materials constraints [1] (i.e. 5–10 MW/m<sup>2</sup> steady state power load). Due to the anomalous character of particle and energy perpendicular transport in the tokamak SOL, no sound theoretical prediction exists for the power flux decay length and, consequently, for the peak power deposition in ITER.

The study of the power flux peak and width scaling can be performed by means of two different sets of measurements, either by using the measured SOL plasma parameters ( $n_e$ ,  $T_e$ ,  $T_i$ ) at the midplane or by

studying the power deposited on the divertor plates measured with Langmuir probes or infrared cameras. The first approach, described in another companion paper [2], has the advantage of not being influenced in its interpretation by the power losses in the divertor and SOL. It has the disadvantage, however, of suffering from uncertainties in the position of the magnetic separatrix and the usual lack of  $T_i$  measurements in the SOL. In this paper, we concentrate in the second approach by utilising measurements of the power deposition by infrared cameras from the major divertor tokamaks. The experimental power deposition database analysed here has been assembled under the supervision of the ITER Divertor Modelling and Database Expert Group within the framework of the ITER-EDA.

## 2. Database: Definitions and analysis

The main objective of this analysis is to understand, in terms of physics variables, the behaviour of the peak

---

\* Corresponding author. Tel.: +49 893299 4219; fax: +49 893299 4312; e-mail: loarte@sat.ipp-garching.mpg.de.

parallel power flux (the actual power on material surfaces depends on the divertor design) so that it can be reliably extrapolated to ITER. Therefore, in principle, we would scale this magnitude from existing experiments by using the measured parallel peak power flux. This approach requires the angle between the divertor tiles and the magnetic field to be accurately known (which is difficult for low angles of incidence of the field onto the divertor) including the real alignment inaccuracies. Therefore, in order to compare results from various experiments, we have resorted to the study of the power flux width scaling, which is less affected by tile misalignments, and from it derive the parallel peak heat flux. In all the analysis performed here we concentrate on the study of the outer divertor (where the largest power fluxes are measured). We also assume that there are no large toroidal asymmetries in the power deposition onto the divertor and, therefore, our measurements are representative of the average divertor power load for all devices. Experimental evidence from several experiments that supports such assumption can be found in Refs. [3–5].

The data contained in the ITER power deposition database come from discharges in ASDEX-Upgrade, DIII-D, JET and JT-60U in Ohmic, L-mode and H-mode regimes. Most of the data contained in it has already been analysed by the different groups, a description of such analyses can be found for ASDEX-Upgrade in Refs. [4,6,7], DIII-D [8–10], JET [11–13] and JT-60U [14–16] together with details of the experimental set-up for each device. In this paper we perform a cross-machine comparison with the aim of determining the size scaling of the power SOL width.

The measured power deposition profiles in most experiments present a sharp decay in the SOL near the separatrix and a flatter part in the outer SOL. Two methods can be used to characterise such profiles, either to fit the steep part of the profile and study its scaling, assuming that it dominates the profile, or to define an integral power width,  $\lambda_q$ :

$$\lambda_q = \frac{\int_{\text{div}} q_{\text{div}} 2\pi R dr}{2\pi R_{\text{div}} q_{\text{div}}^{\text{peak}}} \frac{R_{\text{div}} B_{\theta}^{\text{div}}}{R_{\text{mp}} B_{\theta}^{\text{mp}}}, \quad (1)$$

where  $\lambda_q$  is referred to the outer midplane of the device ( $R_{\text{mp}}$ ),  $q_{\text{div}}$  is the measured power flux onto the target and the second fraction in Eq. (1) accounts for the divertor flux expansion. The second method is more robust for inter-machine comparisons and it will be the one adopted here. It has also the advantage that it takes implicitly into account the real effect of the diffusion of energy into the private flux region that reduces the measured peak power flux.

The power flux width values deduced by these two methods are usually different. Fig. 1 shows the ratio between the power flux widths deduced with the two

methods for ASDEX-Upgrade ELMy H-modes, with the integral value being typically a factor of 1.5–2.5 larger than the exponential one. Ratios in this range are typical for all divertor experiments.

In order to interpret the experimental scaling of the power flux width, a physics based model for the SOL must be used. Here we follow the accepted assumption that the power flux in the SOL is dominated by electron conduction along the field and anomalous transport across it. We further assume that such anomalous transport is described by a diffusion coefficient that depends on plasma parameters:

$$\chi_{\perp} \propto T_e^{\alpha} n_e^{\beta} q_{95}^{\gamma} B_{\phi}^{\delta} R^{\epsilon} Z_{\text{eff}}^{\eta}. \quad (2)$$

Under these assumptions the power flux width scales as

$$\lambda_{\text{div}} \propto P_{\text{SOL}}^{2\alpha-5/9+2\epsilon} n_{\text{SOL}}^{7\beta+7/9+2\epsilon} q_{95}^{4\alpha+7\gamma+4/9+2\epsilon} B_{\phi}^{7\delta/9+2\epsilon} R^{7\epsilon+14/9+2\alpha} Z_{\text{eff}}^{7\eta+2\epsilon+2/9+2\epsilon}, \quad (3)$$

where  $P_{\text{SOL}}$  is the power flux into the SOL,  $n_{\text{SOL}}$  is the separatrix density,  $q_{95}$  is the safety factor and we have taken into account that the parallel electron conductivity decreases as  $Z_{\text{eff}}^{-1}$  [17].

Two problems are encountered with the application of this method: the first one is the need to know the separatrix density  $n_{\text{SOL}}$  and the second one is the accurate determination of  $P_{\text{SOL}}$  and the sharing of the power flow between the divertors, which is dependent on plasma conditions. The standard approach to circumvent these problems is to perform the scalings with the line average density ( $n_{\text{SOL}} \sim \langle n_e \rangle$  assumed) and with the measured power deposited at the plate instead of the SOL power [6,14] (a reasonable approximation for low radiation regimes). Using the measured divertor power also takes implicitly into account other losses that take place in the experiment, such as charge exchange losses, that make the global power balance problematic [4,16].

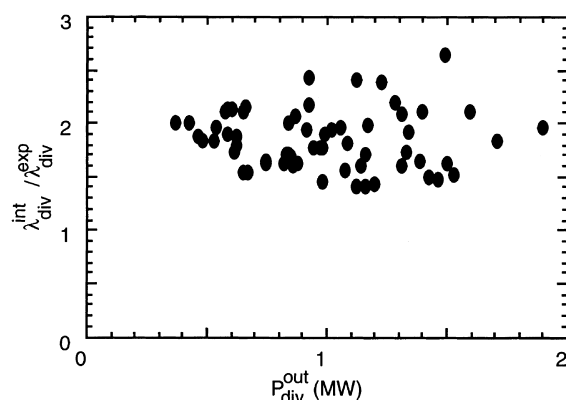


Fig. 1. Ratio of the exponential and integral power flux widths for the outer divertor versus measured divertor power for ASDEX-Upgrade H-modes.

### 3. Power flux width scaling in Ohmic and L-mode discharges

All experiments report that for Ohmic and L-mode discharges the power deposition width increases with plasma density,  $q_{95}$  and decreases with input power [7,8,14]. This last trend is clearly displayed by the data in the ITER power deposition database (Fig. 2). At the higher power end for ASDEX-Upgrade [6,7], DIII-D [8] and JET there is a saturation of the narrowing of the power profile with power, which is not obvious in JT-60U [14].

In principle, we can use in the scaling both the SOL power or the divertor power. The main problem with the SOL power is that it is not well determined in some experiments and, furthermore, the power sharing between the divertors may depend on plasma conditions in different way for various experiments. Part of the difference in the inner/outer target power sharing is due to asymmetric divertor radiation and not to the power flow to either divertor. However, even in low radiation regimes, the target power asymmetry depends on other plasma parameters such as triangularity and  $q_{95}$  [11,12]. For instance, the measured power asymmetry for L-mode discharges in JET [13] and JT-60U [14,15] depends mainly on  $q_{95}$  [13,14] (Fig. 3). Therefore, we have opted to carry out two scalings one with the measured divertor power and other with the total input power, so that any such possible effect is included in the scalings.

The two best scalings found within the database of Ohmic and L-mode discharges are as follows.

*Scaling L-1 (with measured divertor power) (Fig. 4):*

$$\lambda_q^{L-1}(\text{m}) = (6.6 \pm 2.2)10^{-4}R(\text{m})^{1.21 \pm 0.15}$$

$$P(\text{MW})_{\text{div}}^{-0.19 \pm 0.05} q_{95}^{0.59 \pm 0.11} \bar{n}_e (10^{19} \text{m}^{-3})^{0.54 \pm 0.15} Z_{\text{eff,scal}}^{0.61 \pm 0.09}$$

*Scaling L-2 (with total input power):*

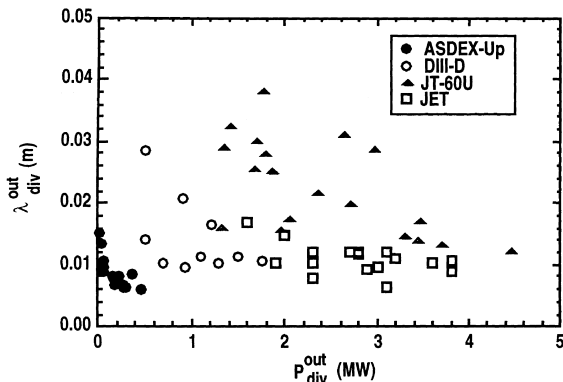


Fig. 2. Measured power deposition width versus outer divertor power for Ohmic and L-mode discharges in the ITER power deposition database.

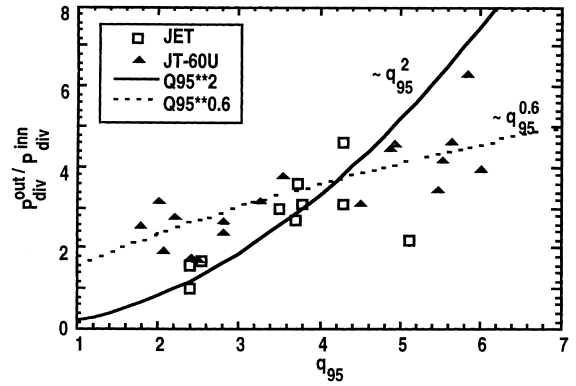


Fig. 3. Measured divertor power asymmetry for JET and JT-60U Ohmic and L-mode discharges. An increase of this asymmetry with  $q_{95}$  is seen in both experiments.

$$\lambda_q^{L-2}(\text{m}) = (7.2 \pm 2.2)10^{-4}R(\text{m})^{1.21 \pm 0.15}$$

$$P(\text{MW})_{\text{TOT}}^{-0.28 \pm 0.08} q_{95}^{0.59 \pm 0.11} \bar{n}_e (10^{19} \text{m}^{-3})^{0.68 \pm 0.16} Z_{\text{eff,scal}}^{0.65 \pm 0.09}$$

Most of the uncertainty in the first coefficient for both scalings comes from the stronger decrease of the power deposition width with power seen in JT-60U [14,15] than in other experiments. The second scaling has a stronger power and density dependence, as expected from the larger radiation losses at higher densities/lower powers (implicit in this scaling). Because of incomplete  $Z_{\text{eff}}$  measurements,  $Z_{\text{eff}}$  has been calculated with the multimachine scaling law in [18]. This calculated value is in good agreement with the available measurements of  $Z_{\text{eff}}$  in the database.

These scalings imply a dependence of  $\chi_{\perp}$  on plasma parameters (Eq. (3)):

$$\chi_{\perp} \propto n_e^{-0.02 \pm 0.04} T_e^{1.17 \pm 0.21} q_{95}^{-0.29 \pm 0.09} R^{-0.01 \pm 0.04} Z_{\text{eff}}^{0.41 \pm 0.06} \quad (4)$$

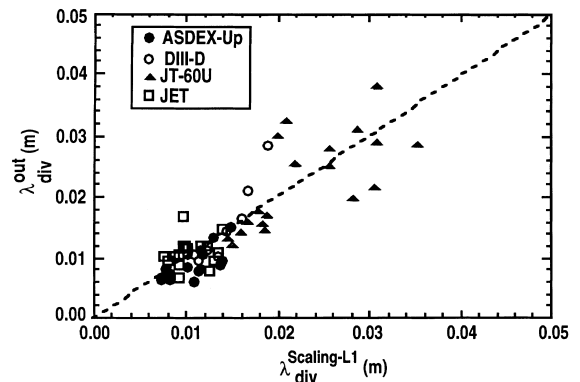


Fig. 4. Measured outer divertor power width for Ohmic and L-modes versus scaling law L-1 for the ITER power deposition database.

with no dependence on toroidal field. From the existing data we can not rule out that the  $q_{95}$  dependence is a consequence of the density peaking with  $q_{95}$  (lower  $n_{sep}$  for the same  $\langle n_e \rangle$  at higher  $q_{95}$ ) seen for example in ASDEX-Upgrade [19]. The scaling in Eq. (4) has a similar  $T_e$  dependence to Bohm transport but without the magnetic field dependence. The trend with  $T_e$  and  $Z_{eff}$  of Eq. (4) is opposite to that found in the analysis of Langmuir probe data from JET and Alcator C-mod [20] where  $\chi_{\perp} \propto T_e^{1.5} Z_{eff}^{-1}$ . If such a scaling were applicable to our experimental database, the power width scaling would be  $\lambda_q \propto P_{ower}^{-4/3} Z_{eff}^{-4/3}$ . Such a strong decrease of the L-mode power width with power has not been reported, the largest one being  $\lambda_q \propto P_{ower}^{-0.49 \pm 0.18}$  for JT-60U [14,15]. This discrepancy could be due to the different diagnostic techniques or to the ion temperature (not measured by Langmuir probes) dominating the power width; further work is needed to clarify this issue.

#### 4. Power flux width scaling in H-mode discharges

We consider only the analysis of the steady state power deposition in ELMy H-modes, the instantaneous ELM power deposition being discussed in a companion paper [21]. The analysis of the power deposition in H-mode discharges is more complex than for L-modes due to the link between confinement and SOL width and of plasma current and plasma density which are closely tied in H-modes, unlike for L-modes. In first place, contrary to the L-modes, most experiments report an increase of power flux width with input power for H-modes, the dependence on the power in some cases being weak but positive [6,10,16] (Fig. 5). In principle, this could be attributed to the averaging effect of the ELMs on the power profile. However, the power deposition data for ELMy H-modes reveals that during ELMs most of the

power flows to the inner divertor. At the outer divertor, ELMs do not change substantially the shape of the profile [7,9]. This is borne by the JT-60U ELM-free H-modes which show a similar behaviour to that of ELMy H-modes from ASDEX-Upgrade and DIII-D (Fig. 5).

A similar scaling approach to that followed for L-modes is not applicable for H-modes, due to the colinearity of some of the variables used in the scaling. In order to minimise the differences among the data analysed, we have selected a subset of discharges with no gas puff, so that they have similar confinement. The analysis of such set yields that the dominant variables in the H-mode power width scaling are the input power (or power to the divertor),  $q_{95}$  and the toroidal field (the density is linked to them in ELMy H-modes) with no dependence on the size of the device. The best scalings obtained for this set are as follows.

*Scaling H-1 (with measured divertor power) (Fig. 6):*

$$\lambda_q^{H-1}(\text{m}) = (5.2 \pm 1.3) 10^{-3} P_{div}^{0.44 \pm 0.04} B(T)_{\phi}^{-0.45 \pm 0.07} q_{95}^{0.57 \pm 0.16}$$

*Scaling H-2 (with total input power):*

$$\lambda_q^{H-2}(\text{m}) = (5.3 \pm 1.4) 10^{-3} P_{TOT}^{0.38 \pm 0.04} B(T)_{\phi}^{-0.71 \pm 0.08} q_{95}^{0.30 \pm 0.15}$$

Similar trends have been found previously in DIII-D [9] and scalings of this type have been first reported for ASDEX-Upgrade alone [6] in similar discharges, the sign of the dependence on power for H-modes being opposite to that found for L-modes. Due to the interrelation of many plasma parameters in H-modes, these scalings cannot be used to deduce first principle dependences of  $\chi_{\perp}$  in this regime. For instance, the density of ELMy H-modes tends to be a fixed fraction of the Greenwald limit (typically ~60% for most of the data in this database), which scales as  $I/R^2$ . Therefore some of

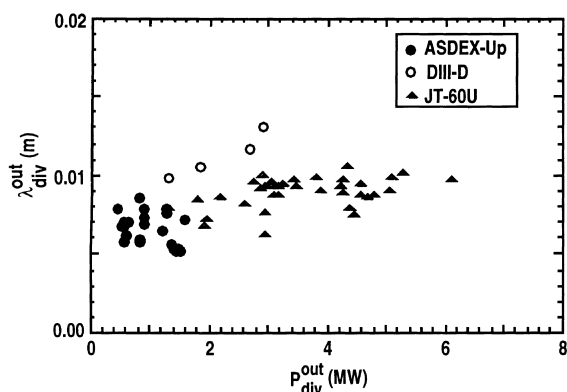


Fig. 5. Measured power deposition width versus divertor power for H-mode discharges without gas puff in the ITER power deposition database.

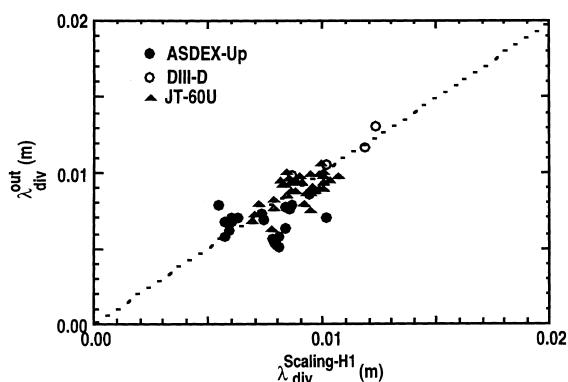


Fig. 6. Measured outer divertor power width for H-modes versus scaling law H-1 for the ITER power deposition database.

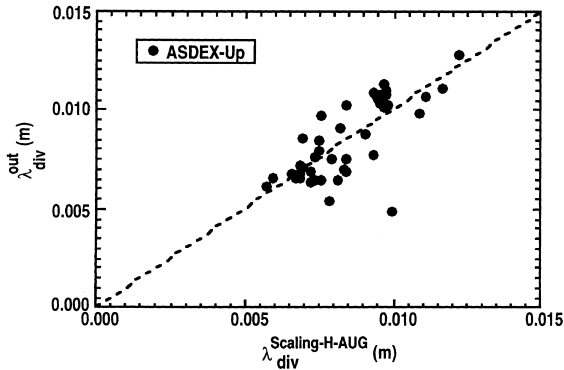


Fig. 7. Measured outer divertor power width for ASDEX-Upgrade ELMy H-mode gas scan versus scaling law H-AUG for the ITER power deposition database.

the trends in the above scalings could be attributable to a density dependence.

The influence of confinement deterioration on the measured power width has been analysed with ASDEX-Upgrade data for density (gas puff) scans in H-mode; at lower confinement the power width increases and returns to values typical of high density L-modes. Scaling for ASDEX-Upgrade of such relation yields (Fig. 7):

$$\lambda_q^{\text{Scaling-H-AUG}} \text{ (m)} = (3.5 \pm 0.9) 10^{-3} P_{\text{div}}^{0.23 \pm 0.08} q_{95}^{0.69 \pm 0.14} H_{89}^{-0.88 \pm 0.22}.$$

Similar trends have been reported for the SOL density and temperature fall-off lengths in ASDEX-Upgrade ELMy H-modes [19].

Other internal dependences among parameters that influence the results for the scaling in H-modes is that of the ratio of the separatrix density to the line average density. This ratio scales with power and  $q_{95}^{-0.5}$ , as it has been reported from DIII-D [9] and ASDEX-Upgrade [19] and, therefore, part of the  $q_{95}$  dependence in the scalings H-1 and H-2 may be due to this effect.

### 5. Conclusions

In this paper we have summarised the analysis of the ITER power deposition database. The trends for the power deposition width with plasma parameters found in most experiments seem to be in good qualitative agreement and reasonable quantitative agreement. For Ohmic and L-mode discharges the power width decreases with power and increases with density,  $q_{95}$  and the size of the device. This can be understood in terms of a Bohm-like transport coefficient at the plasma edge, under these conditions. For H-mode discharges all experiments show a broadening of the power deposition profile with increasing power and  $q_{95}$ . This effect may not be a consequence of anomalous transport itself but of the interrelation between several plasma parameters (density, current, separatrix density and confinement) in H-modes. Therefore the scalings obtained for this regime can be considered only as effective scalings; it is not clear if the effects that lead to such scalings can be extrapolated to ITER. The extrapolation of the above scalings to the ITER-EDA machine ( $R = 8.14$  m,  $I_p = 21$  MA,  $B_\phi = 5.7$  T,  $q_{95} = 3.0$ ,  $Z_{\text{eff}} = 1.8$ ) would give the results shown in Table 1; where the magnetic and divertor geometry of ITER have been taken into account. The L-mode plasma parameters are reasonable guesses without detailed calculations to justify them. It is not surprising that both L- and H-mode scaling laws produce a similar value of the extrapolated peak power for ITER, as this is indeed seen in the raw experimental data. The values of  $\lambda_q$  found at the higher power end for L-mode and H-modes in Figs. 2 and 5 are very similar, although obtained at very different densities and input powers. The values obtained for ITER show that if the density and calculated levels of radiation can be achieved in such a device, the peak power flux falls within reasonable engineering limits and in agreement with code calculations [22], i.e. the scaled power flux width remains broad enough even for these conditions. Further work is necessary to verify if at such high

Table 1  
Extrapolated values of power flux peak and width for ITER-EDA from the scalings derived in this paper

Regime	$\langle n_e \rangle$ ( $10^{19} \text{ m}^{-3}$ )	$P_{\text{net}}$ (MW)	$P_{\text{div}}$ (MW)	$\lambda_q$ (cm)	$P_{\parallel}^{\text{peak}}$ ( $\text{MW}/\text{m}^2$ )	$P_{\text{div}}^{\text{peak}}$ ( $\text{MW}/\text{m}^2$ )
L-mode (L-1)	5.0	100	40	$2.7 \begin{pmatrix} +0.8 \\ -0.8 \end{pmatrix}$	$61 \begin{pmatrix} +26 \\ -14 \end{pmatrix}$	$2.2 \begin{pmatrix} +0.9 \\ -0.5 \end{pmatrix}$
L-mode (L-2)	5.0	100	40	$2.1 \begin{pmatrix} +0.9 \\ -0.7 \end{pmatrix}$	$79 \begin{pmatrix} +40 \\ -24 \end{pmatrix}$	$2.9 \begin{pmatrix} +1.5 \\ -0.9 \end{pmatrix}$
H-mode (H-1)	10.0	200	50	$2.5 \begin{pmatrix} +0.2 \\ -0.2 \end{pmatrix}$	$83 \begin{pmatrix} +7 \\ -6 \end{pmatrix}$	$3.0 \begin{pmatrix} +0.3 \\ -0.2 \end{pmatrix}$
cH-mode (H-2)	10.0	200	50	$1.6 \begin{pmatrix} +0.2 \\ -0.2 \end{pmatrix}$	$129 \begin{pmatrix} +18 \\ -14 \end{pmatrix}$	$4.7 \begin{pmatrix} +0.7 \\ -0.5 \end{pmatrix}$

densities as in ITER (~100% of the Greenwald limit) our experimental H-mode scaling laws (deduced for discharges at ~60% of the Greenwald limit) remain valid.

The results obtained so far call for dedicated experiments to be carried out in all devices in order to reduce the statistical errors of the scaling laws presented in this paper. The fact that the basic dependences are similar in all devices provides a reasonable chance for the success of such approach.

### Acknowledgements

The authors wish to acknowledge fruitful discussions with members of the ITER Divertor Modelling and Database Expert Group and ITER Divertor Physics Expert Group. The database used in the present analysis was supplied by tokamak teams all over the world: ASDEX-Upgrade, DIII-D, JT-60U and JET. The authors wish to express their sincere thanks to all members of these teams. Computational support by the IPP Computing Department and the computer support staff of the ITER Garching JWS is also acknowledged.

### References

- [1] R. Parker, et al., *J. Nucl. Mater.* 241–243 (1997) 1.
- [2] K. McCormick et al., these Proceedings.
- [3] R.D. Monk, Ph.D. Thesis, University of London, 1996.
- [4] A. Herrmann, et al., in: Proceedings of the 24th EPS Conf. Cont. Fusion Plasma Phys., 21A (IV) (1997) 1417.
- [5] A. Leonard, et al., *J. Nucl. Mater.* 241–243 (1997) 628.
- [6] A. Herrmann, et al., in: Proceedings of the 23rd EPS Conf. Cont. Fusion Plasma Phys., 20C (II) (1996) d-039.
- [7] C.S. Pitcher, et al., *Plasma Phys. Control. Fusion* 39 (1997) 1129.
- [8] D.N. Hill, et al., *J. Nucl. Mater.* 176–177 (1990) 158.
- [9] D.N. Hill, et al., *J. Nucl. Mater.* 196–198 (1992) 204.
- [10] D. Buchenauer, et al., *J. Nucl. Mater.* 196–198 (1992) 133.
- [11] S. Clement, et al., in: Proceedings of the 22nd EPS Conf. Cont. Fusion Plasma Phys., 19C (III) (1995) 301.
- [12] S. Clement, et al., in: Proceedings of the 23rd EPS Conf. Cont. Fusion Plasma Phys. 20C (I) (1996) a-055.
- [13] A.V. Chankin, et al., *Plasma Phys. Control. Fusion* 38 (1996) 1579.
- [14] K. Itami, et al., *J. Nucl. Mater.* 196–198 (1992) 755.
- [15] K. Itami, et al., *Plasma Phys. Control. Fusion Res.* 1 (1992) 391.
- [16] K. Itami, et al., *J. Nucl. Mater.* 220–222 (1995) 203.
- [17] S.I. Barginskii, in: M.A. Leontovich (Ed.), *Review of Plasma Physics*, vol. 1, Consultants Bureau, New York, 1965.
- [18] G. Matthews, et al., *J. Nucl. Mater.* 241–243 (1997) 450.
- [19] J. Schweinzer, et al., in: Proceedings of the 24th EPS Conf. Cont. Fusion Plasma Phys. 21A (IV) (1997) 1449.
- [20] S.K. Erents, et al., in: Proceedings of the 24th EPS Conf. Cont. Fusion Plasma Phys. 21A (I) (1997) 121.
- [21] A. Leonard et al., these Proceedings.
- [22] H.D. Pacher et al., these Proceedings.